

# Ligand Fields from Misdirected Valency. 1. Lone-Pair Contributions in Planar Cobalt(II) Schiff-Base Complexes<sup>†</sup>

Robert J. Deeth, Melinda J. Duer, and Malcolm Gerloch\*

Received January 3, 1986

Ligand-field analyses leading to the reproduction of the  $g$  tensors of two low-spin, planar-coordinated cobalt(II) complexes are reported. The electron spin resonance data in both systems are characterized by one principal  $g$  value being much larger than the other two and lying in the coordination plane. The maximum  $g$  value lies parallel to the approximate diad in Co(salen) (salen =  $N,N'$ -ethylenebis(salicylideneaminato)) but at right angles to this in Co(clamben) (clamben =  $N,N'$ -ethylenebis(2-amino-5-chlorobenzylideneaminato)). This reversal is interpreted within the present analyses in terms of a ligand-field contribution from the nonbonding, lone-pair electrons on the oxygen donors of the salen chelate. Both complexes display marked nephelauxetic effects that are associated with strong ligand  $\sigma$  donation together with weak  $\pi$  acidity normal to the chelate planes.

## 1. Introduction

Contemporary ligand-field analyses have addressed the chemical significance of parameters obtained through the superpositional approach known as the angular overlap model (AOM). A seemingly central axiom<sup>1-3</sup> of the AOM is that each local perturbation of the metal  $d(f)$  electrons is diagonal, so that  $\sigma$  and  $\pi$  metal-ligand interactions may be separated clearly. Yet Schäffer<sup>1</sup> himself recognized that the assumption may not be necessary and would be broached by what Liehr<sup>4</sup> had earlier referred to as "misdirected valency". For local pseudosymmetry of any metal-ligand bonding that is significantly less than  $C_{2v}$ , nonzero, off-diagonal ligand-field matrix elements arise and serve to blur the chemical simplicity of the whole approach. Although very many ligands do present a relatively high-symmetry local environment, there remain numerous examples of a less than "ideal" ligand alignment. Perhaps the first to be identified arose in earlier applications of the AOM to the paramagnetism and spectroscopy of a tetrahedral<sup>5</sup> and of a nominal square-pyramidal, five-coordinate<sup>6</sup> Schiff base complex of nickel(II). These analyses were characterized by significant values for in-plane Ni-O  $\pi$  interaction but zero values for the corresponding Ni-N imine  $\pi$  perturbation. No in-plane  $\pi$  orbitals of reasonably accessible energy are expected for either donor atom, of course. It was suggested<sup>6</sup> that the nonzero parameter value for the oxygen donor ultimately derived from the presence of the nonbonding, nominal  $sp^2$  lone pair. Although the parameterization scheme in these early studies was inadequate, this different aspect of Liehr's misdirected valency was apparent. Since then we have frequently suspected the importance of such ligand-field contributions, and several parameterization schemes have been capable of sustaining appropriate nonzero, off-diagonal local parameters. It has not been possible, however, to provide an *unequivocal* demonstration of the effect because of the ill determinancy of most ligand-field studies characterized by this extra degree of freedom.

We are now able to do so. In this series we present ligand-field analyses of three different groups of complexes that, we believe, establish the phenomenon beyond doubt. We have sought out examples in which the effect is to be expected in principle and for which the most "conventional" or restricted parameterization schemes are first shown to be quite inadequate.

## 2. The Cellular Ligand-Field Parameter, $e_{\pi\sigma}$

Gerloch and Woolley<sup>2,3,7,8</sup> have explored the structure of ligand-field theory and of its cellular modeling originally called the AOM. We have recently felt obliged to rename the ligand-field version of the AOM that we have always used, referring now to the cellular ligand-field (CLF) model; reasons for the new name are discussed fully elsewhere.<sup>9</sup> Studies of the AOM—and hence of the CLF model also—describe ligand-field matrix elements as dominated by a so-called "dynamic" component of the form

$$V_{ij}(\text{dynamic}) \sim \sum_x \left\langle d_i \left| \frac{V^i|\chi\rangle\langle\chi|V^j}{\epsilon_d - \bar{\epsilon}_x} \right| d_j \right\rangle \quad (1)$$

The  $d$  functions are eigenfunctions of the mean Hamiltonian in the given complex, and so their radial character changes from molecule to molecule. The  $\chi$ 's—the so-called "bond-orbitals"—are similarly self-selected by the system at hand and represent those parts of ligand functions that are involved in significant bond formation together with metal functions, which predominantly comprise  $s$  and/or  $p$  orbitals in the usual Werner complexes subjected to ligand-field study. The  $\chi$ 's are not to be considered as metal and ligand function bases prior to molecule formation but rather as spatially local orbitals arising after appropriate electron redistribution throughout the complex as a whole has taken place in response to the usual requirements of chemistry and the electroneutrality principle. Only by recognition of such concepts can ligand-field theory and the CLF model achieve self-consistency.

In the most usual circumstances where local metal-ligand interactions can be considered as possessing essentially  $C_{2v}$  pseudosymmetry, the  $\chi_\lambda$ 's are characterized by  $\lambda = \sigma, \pi_x, \pi_y$  and the  $V_{ij}$ 's are diagonal in the local frame. Both AOM and CLF approaches then refer to  $e_\lambda$  parameters whose (major) dynamic components take following the form in the CLF:

$$e_\lambda(\text{dynamic}) \sim \sum_x \left\langle d_\lambda \left| \frac{V^i|\chi\rangle\langle\chi|V^j}{\epsilon_d - \bar{\epsilon}_x} \right| d_\lambda \right\rangle \quad (2)$$

$$= \sum_x \frac{|\langle d_\lambda | V^i | \chi \rangle|^2}{\epsilon_d - \bar{\epsilon}_x} \quad (3)$$

The potential  $V^i$  transforms as  $\Gamma_1$  in the local cell, of course, and arises from the nonspherical part of the electron density in that region. The major contribution to  $V^i$  will derive from electrons that lie closest to the  $d$  functions, and hence  $V^i$  is dominated by the bonding electrons themselves.<sup>29</sup> The cellular potential is common to all local matrix elements; that is for a given ligand  $l$ , it is common for all  $\lambda$ . As the numerator in (3) is necessarily real positive, the signs of empirical, diagonal  $e_\lambda$  parameters are determined by the signs of the denominators. When the energy of the bonding orbital is less than that of the  $d$  orbitals—as will usually obtain for ligands in donor modes— $\epsilon_d > \bar{\epsilon}_x$  and  $e_\lambda$  is positive. Negative  $e_\pi$  parameters are associated with dominant contributions to the dynamic term in which  $\chi$  lies higher in energy

(1) Schäffer, C. E. *Struct. Bonding (Berlin)* 1968, 5, 68.

(2) Gerloch, M.; Harding, J. H.; Woolley, R. G. *Struct. Bonding (Berlin)* 1981, 46, 1.

(3) Gerloch, M. *Magnetism and Ligand-Field Analysis*; Cambridge University Press: Cambridge, U.K., 1983.

(4) Liehr, A. D. *J. Phys. Chem.* 1964, 68, 665.

(5) Cruse, D. A.; Gerloch, M. *J. Chem. Soc., Dalton Trans.* 1977, 152.

(6) Cruse, D. A.; Gerloch, M. *J. Chem. Soc., Dalton Trans.* 1977, 1613.

(7) Woolley, R. G. *Mol. Phys.* 1981, 42, 703.

(8) Gerloch, M.; Woolley, R. G. *Prog. Inorg. Chem.* 1983, 31, 371.

(9) Deeth, R. J.; Gerloch, M.; Woolley, R. G., in preparation.

<sup>†</sup>No reprints available from this laboratory.

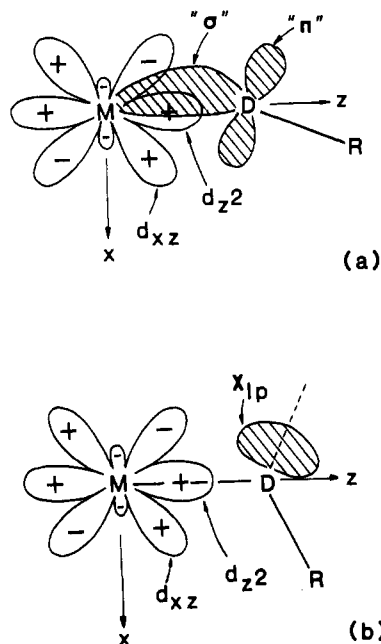


**Figure 1.** (a) Illustration of how bent  $\sigma$  and  $\pi$  bonds between metal (M) and donor atoms (D) require a local ligand-field matrix element connecting  $d_{\sigma}$  and  $d_{\pi}$  orbitals. (b) Same interaction arising via the agency of a nonbonding, lone-pair orbital,  $\chi_{lp}$ , on the ligand. For the given local frames, both forms of misdirected valency require positive values of  $e_{\pi\sigma}$  for donor orbitals; see section 2.

than the d orbitals. This will usually correspond to the  $\chi$  being a formally empty bonding function but this vacancy does not mean that  $e_{\pi}$  must be small, for, as above,  $V'$  arises from the electron density in occupied orbitals and is the same for all  $e_{\lambda}$ . (The case for negative  $e_{\sigma}$  parameters being associated with coordination voids formed the subject matter of ref 10.) Often only one bond orbital will lie energetically close enough to the d orbitals in the complex to make a significant contribution to the sum in (2). Occasionally, however, two such functions may be important: for example, if both  $\pi$  and  $\pi^*$  ligand functions (HOMO and LUMO-like functions in the language of frontier orbital theory) are close, the resultant  $e_{\pi}$  parameter will monitor their net contribution. Altogether—though one must bear in mind the sum in (2)—the signs of diagonal, local matrix elements like  $e_{\sigma}$ ,  $e_{\pi x}$ , and  $e_{\pi y}$  are determined by the denominators in the expression.

Now consider the situation that arises when the local pseudo-symmetry no longer approximates  $C_{2v}$ . Two common circumstances are depicted in Figure 1, corresponding to a bent bond as originally envisaged by Liehr (a) and to the perturbation by a nonbonding lone pair (b). As usual, define  $z$  as directed from the metal to the donor atom and let the normal to the plane of the bent bond or lone pair define  $y$ . Envisaging no perturbation of the local  $d_{x^2-y^2}$  and  $d_{xy}$  orbitals, as conventional, we then consider  $d_{yz}$  transforming uniquely as  $a''$  in  $C_3$  with  $d_{xz}$  and  $d_{z^2}$  transforming as  $a'$ . The corresponding ligand-field matrix in the local  $C_3$  symmetry takes the form

$$\begin{array}{cccc} & d_{z^2} & d_{xz} & d_{yz} \\ d_{z^2} & e_{\sigma} & e_{\pi\sigma} & 0 \\ d_{xz} & e_{\pi\sigma} & e_{\pi x} & 0 \\ d_{yz} & 0 & 0 & e_{\pi y} \end{array} \quad (4)$$

The misdirected ligand orbital thus connects  $d_{z^2}$  and  $d_{xz}$ , and the dynamic contribution to the off-diagonal parameter  $e_{\pi\sigma}$ , corresponding to (2), is now given by

$$e_{\pi\sigma}(\text{dynamic}) \sim \sum_x \left\langle d_{xz} \left| \frac{V|\chi\rangle\langle\chi|V'}{\epsilon_d - \bar{\epsilon}_x} \right| d_{z^2} \right\rangle \quad (5)$$

When the effect derives from a lone pair as in Figure 1b the sum

in (5) comprises just one term: in the case of a formal  $\sigma$  and  $\pi$  donor as depicted in Figure 1a, the sum is over two parts arising from the bond orbital formed between metal (s and/or p) orbitals and the ligand  $\sigma$  function and from that formed with the ligand  $\pi$  orbital.

The sign of  $e_{\pi\sigma}$ , unlike that for a diagonal element, can be affected by both numerator and denominator in (5). The d orbitals in bra and ket, though necessarily belonging to the same irreducible representation, are different and may, or may not, be in phase. We define the numerator of  $e_{\pi\sigma}$  as positive when the ligand  $\sigma$  lobe—or nonbonding lone pair, as appropriate—lies in the negative quadrant of the  $xz$  plane of Figure 1, as shown. This seemingly counterintuitive definition arises as follows. Consider, for simplicity but without any essential loss, the case of a ligand offering only “ $\sigma$ ” donation to the metal but misdirected so that the local off-diagonal  $e_{\pi\sigma}$  parameter becomes nonzero: assume also, for simplicity, that the diagonal  $\pi_x$  element approximates zero. In the frame of Figure 1, and in the  $xz$  plane, the local ligand-field matrix assumes the form

$$\begin{array}{ccc} & d_{z^2} & d_{xz} \\ d_{z^2} & e_{\sigma} & e_{\pi\sigma} \\ d_{xz} & e_{\pi\sigma} & 0 \end{array} \quad (6)$$

eigenfunctions for which are

$$E_{\pm} = (e_{\sigma} \pm (e_{\sigma}^2 + 4e_{\pi\sigma}^2)^{1/2})/2 \quad (7)$$

Considering misdirected valence as a small perturbation, so that  $e_{\pi\sigma} < e_{\sigma}$ , implies that the larger root  $E_+$  is associated with the  $\sigma$  interaction in the frame that diagonalizes (6). The corresponding eigenvector in the frame of Figure 1 and (6) is

$$(e_{\sigma} - E_+)c_{z^2} - e_{\pi\sigma}c_{xz} = 0 \quad (8)$$

in an obvious notation, and this describes a function directed more into the negative  $xz$  quadrant of Figure 1 when  $e_{\pi\sigma}$  is positive.<sup>30</sup> The greater the magnitude of  $e_{\pi\sigma}$ , the greater the displacement of the d orbital hybrid (8) from the  $z$  axis. In turn, a larger magnitude for  $e_{\pi\sigma}$  is to be associated with a greater proximity of the bent bond or lone pair with the metal d hybrid. Exactly opposite signs for  $e_{\pi\sigma}$  parameters would arise if the energy denominator of (5) were negative, but that situation is not expected for the donor qualities of either Liehr's bent bonds or for the occupied lone pairs envisaged in Figure 1. On the other hand, the magnitude of the energy denominator for a lone-pair perturbation is likely to be less than that for bent bonding as the mean energy  $\bar{\epsilon}_x$  of an orbital describing metal–ligand bonding is probably less than that of a lone pair not so engaged.

Elsewhere<sup>3,11</sup> we have described how a nonzero, local matrix element  $\langle d_{xz} | V_{LF} | d_{z^2} \rangle$  begets nonzero components  $Y_1^2$  and  $Y_1^4$  in the local potential: their contributions to the global ligand-field potential for the whole complex are then readily computed by standard methods.<sup>3,11</sup>

### 3. Orientations of g Tensors in Low-Spin, Schiff-Base Complexes of Cobalt(II)

Planar-coordinated, low-spin complexes of cobalt(II) with a wide variety of Schiff-base ligands have long held interest as agents for reversible oxygen uptake. Physical studies on them have centered upon ESR  $g$  values in particular but on bulk susceptibilities also. Two broad classes of complexes are shown schematically in Figure 2, corresponding to donor atom sets  $O_2N_2$  and  $N_2N'_2$ . In an extensive review of the field, Daul et al.<sup>12</sup> list  $g$  values for many complexes in these series, most of which have been determined from powdered samples or from partially orientated molecules in liquid crystals; in a few cases only, detailed single-crystal ESR work on molecules doped into nickel(II) analogues have been reported. Ranges for  $g$  values for the two classes of planar complex are included in Figure 2. In all cases the  $g$  tensors are characterized by one  $g$  value being much larger than the other

(11) Gerloch, M.; McMeeking, R. F. *J. Chem. Soc., Dalton Trans.* **1975**, 2443.

(12) Daul, C.; Schläpfer, C. W.; von Zelewsky, A. *Struct. Bonding (Berlin)* **1979**, *36*, 129.

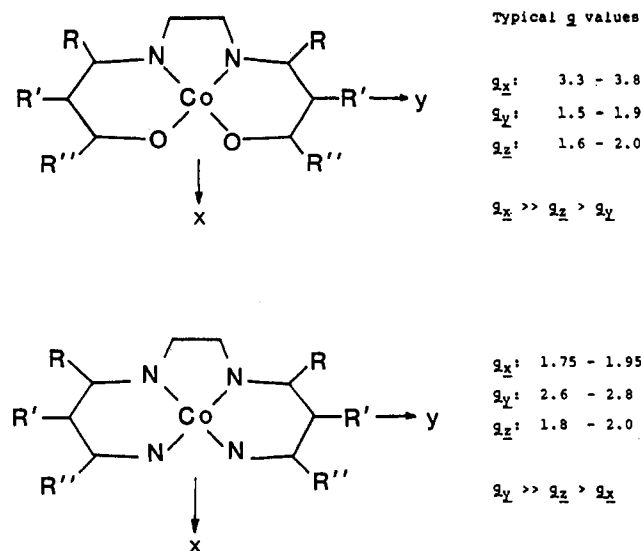


Figure 2. Typical  $g$  values for  $\text{CoN}_2\text{O}_2$  and  $\text{CoN}_2\text{N}'_2$  low-spin, planar complexes.<sup>12</sup>

two and lying in the coordination plane; similar patterns have been found<sup>13</sup> in other planar, low-spin cobalt(II)  $g$  tensors. Some controversy attaches to the orientation of the large  $g$  value in the coordination plane of the Schiff base complexes, however. While the labeling given in Figure 2 is established beyond doubt in a few of the  $\text{CoO}_2\text{N}_2$  species from single crystal work, no similarly unequivocal results are available for the  $\text{CoN}_2\text{N}'_2$  systems. It has been *supposed* that complexes in this group have  $g$  tensors similar to those in the former, but we consider this unlikely. Our assertion arises partly out of the ligand-field calculations detailed in the following section but mostly from the susceptibility anisotropy work of Murray and Sheahan<sup>14</sup> on Co(clamben),  $\text{CoN}_2\text{N}'_2$ , crystals (we follow the nomenclature of Daul et al.<sup>12</sup>), who established that one molecular susceptibility is much larger than the other two and lies along the  $y$  axis in Figure 2. The result strongly implies that the principal  $g$  value parallel to  $y$  should also be the large one, a conclusion that is entirely supported by the calculations reported below. Accordingly, the  $g$  values given in Figure 2 are labelled to reflect the susceptibility tensor and we observe qualitatively *different* eccentricities of the  $g$  tensors for the two classes of complex involving  $\text{N}_2\text{O}_2$  and  $\text{N}_2\text{N}'_2$  coordination.

#### 4. Ligand-Field Analyses

Ligand-field calculations for low-spin cobalt(II) systems require simultaneous consideration of both spin quartets and spin doublets. All results discussed in this paper derive from computations<sup>15</sup> within the full 120-fold basis of the  $d^7$  configuration expressed as free-ion states in  $|J, M_J\rangle$  quantization and diagonalized under the ligand-field Hamiltonian<sup>3</sup>

$$\mathcal{H}_{\text{LF}} = \sum_{i < j} U(i, j) + \sum_i V_{\text{LF}}(\mathbf{r}_i) + \zeta \sum_i \mathbf{l}_i \cdot \mathbf{s}_i \quad (9)$$

in which the Coulomb-like operator gives rise to the usual Condon-Shortley  $F_2$  and  $F_4$  parameters, the ligand-field potential gives rise to CLF $\{e\}$  parameters, and  $\zeta$  is the effective one-electron spin-orbit coupling coefficient. Subsequent perturbation methods, described elsewhere,<sup>3,11</sup> using the magnetic moment operator  $\mu_a = (k\mathbf{l}_a + 2s_a)$ , where  $k$  is Stevens' orbital reduction factor, were used to compute the principal values and orientations of the  $g$  tensors, which together provide the experimental data base. Despite the relatively lengthy nature of such calculations, their well-known sensitivity to quite modest changes in all parameters renders recourse to analytical perturbation expressions established within various restricted bases wholly unreliable. Similarly, we

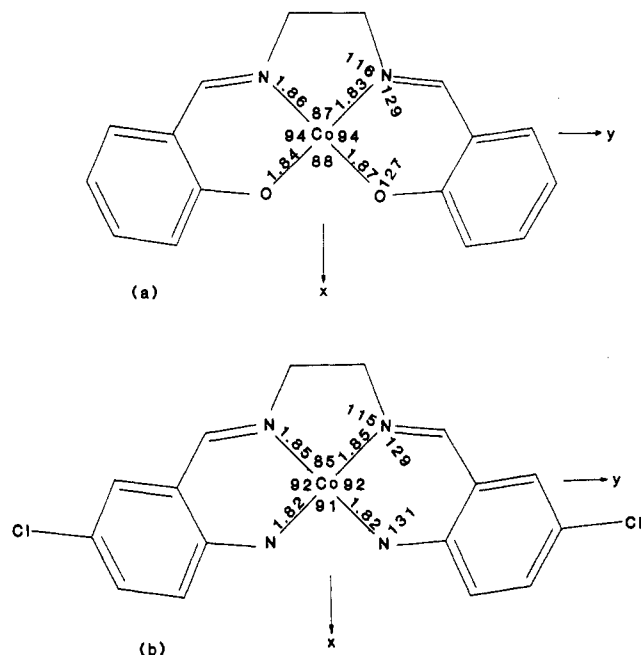


Figure 3. Selected features of the coordination geometry in (a) Co(salen),<sup>16</sup> which suffers a very slight tetrahedral distortion, and (b) Co(clamben),<sup>17</sup> in which the metal atom lies 0.1 Å out of the coordination plane.

have found that significant results upon which chemical understanding can be based must explicitly recognize detailed molecular geometry rather than rely upon higher symmetry idealizations. All calculations here, therefore, take reported atomic coordinates from X-ray analyses<sup>16,17</sup> as input. Some useful structural details of the two Schiff-base complexes studied—representative of the two classes of coordination—are summarized in Figure 3.

**The Salen Complex.** Our analysis seeks to reproduce the observed<sup>12</sup>  $g$  tensor whose principal directions lie close to the approximate diads in this nearly square-coordinated complex: experiment gives  $g_x = 3.81$ ,  $g_z = 1.74$ , and  $g_y = 1.66$ . Wide ranges of all parameter values have been considered as follows: for  $\bar{e}_\sigma(\text{O,N})$ , the mean  $e_\sigma$  value for the essentially holohedrally related oxygen and nitrogen ligators, 5000–10000  $\text{cm}^{-1}$ ; for  $e_\sigma(\text{void})$ , relating to each coordination void (above and below the  $\text{CoO}_2\text{N}_2$  plane),  $-2000$  to  $-6000$   $\text{cm}^{-1}$ ; for  $\bar{e}_{\sigma\perp}(\text{O,N})$ , referring to metal-ligand  $\pi$  interaction perpendicular to the coordination plane,  $-2500$  to  $+2500$   $\text{cm}^{-1}$ ; for  $e_{\pi\parallel}(\text{O})$  and Co–O  $\pi$  bonding in that plane,  $-1000$  to  $+1000$   $\text{cm}^{-1}$ ; for  $e_{\pi\sigma\parallel}(\text{O})$ , describing misdirected valency in the donor atom plane, initially zero and then from  $-3500$  to  $+3500$   $\text{cm}^{-1}$ ; values for  $F_2$ ,  $F_4$ ,  $\zeta$  and  $k$  were varied between 10% and 100% of their free-ion values.

The most apparent characteristic of ligand-field calculations on low-spin, planar-coordinated  $d^7$  systems is the extremely variable response of the model to most parameters as so many levels—both spin doublets and spin quartets—cross, recross, and approach the ground state. Similar behavior was noted<sup>13</sup> in our analysis of the planar, low-spin complex *trans*-dimesitylbis(diphenylethylphosphine)cobalt(II). For most regions of parameter space, the system possesses a well-isolated spin-doublet or spin-quartet ground state and response to parameter variation is fairly flat. Between these plateaulike regions exist steep and complex areas where small alterations in the model give rise to dramatic changes in calculated properties. The present complexes fall into these sensitive regions.

The progress of the analysis is reviewed under three main headings, each associating a stepwise approach to the reproduction of the experiment with distinct physical circumstances. First, the

(13) Falvello, L. R.; Gerloch, M. *Inorg. Chem.* **1980**, *19*, 472.

(14) Murray, K. S.; Sheahan, R. M. *J. Chem. Soc., Chem. Commun.* **1975**, 475.

(15) CAMMAG2, a Fortran program by A. R. Dale, M. J. Duer, M. Gerloch, and R. F. McMeeking.

(16) Schäffer, W. P.; Marsh, R. E. *Acta Crystallogr., Sect. B: Struct. Crystallogr. Cryst. Chem.* **1969**, *B25*, 1675.

(17) Karlsson, R.; Engelhardt, L. M.; Green, M. *J. Chem. Soc., Dalton Trans.* **1972**, 2463.

correct spin state of the complex—and hence the correct order of magnitude of the  $g$  values—is achieved only for very low values of the Condon–Shortly parameters. Precedents for this are to be found in the mesityl complex<sup>13</sup> above and in an analysis<sup>18</sup> of a low-spin, distorted tetrahedral nickel(II) phosphine complex. We find also that the reduction in  $F_2$  from the free-ion value is proportionately greater than that in  $F_4$ , and this too accords with previous experience.<sup>19–21</sup> As expected, rather larger ligand-field parameter values accompany the low-spin state in this system. It is apparent that the penalty exacted in terms of increased pairing energy on transition from a high-spin configuration is very much less than usually suggested; we will return to this point later.

Second, all calculations with  $e_{\pi||} = 0$  failed signally to reproduce the observed orientation of the  $g$  tensor; in particular, the largest  $g$  value was computed to lie parallel to  $y$  (Figure 2) rather than  $x$ , as observed. In this respect at least we concur with Ceulemans et al.<sup>22</sup> (vide infra). We do not agree that the failure of the simple model arises from a neglect of “phase-coupled” ligators, however, and discuss this important question elsewhere.<sup>9</sup> As usual, in applications of the CLF approach, we look for features of the electron density in the coordination shell that may require explicit recognition within a ligand-field analysis. In the present system, we find that density provided by the nonbonding lone pair on each donor oxygen atom. Its ligand-field consequences are parameterized by  $e_{\pi||}(\text{O})$ , as discussed in section 2. A major feature of the present analysis is that inclusion of a nonzero value for this parameter successfully reproduces the observed sense of the primary  $g$  tensor anisotropy.

Finally and third, detailed duplication of the experiment has proved extraordinarily difficult. One might expect that so large a number of variables as are at our disposal here would easily provide for the reproduction of the observed  $g$  tensor and possibly yield few certainties. Yet the correct reproduction of the sense of the secondary anisotropy,  $g_z > g_y$ , emerges as a sufficiently exacting task that we are able to identify an essentially unique set of fitting parameters. The parametric feature that establishes the observed secondary anisotropy is that  $e_{\pi||}(\text{O}) > 0$  and  $e_{\pi\perp}(\text{O}, \text{N}) < 0$ .

Parameter values affording detailed reproduction of experimental  $g$  tensor are not completely unique but lie within fairly narrow bounds in a correlated manner. That fitting region is narrowed markedly, however, by reference to the optical d–d transition energies in the complex. Hitchman<sup>23</sup> reports features at 3900, 8300, and  $>17000 \text{ cm}^{-1}$  with extinction coefficients of 65, 16, and  $>1000 \text{ mol}^{-1} \text{ L cm}^{-1}$ , respectively. Now, within the correlated parameter space defining good reproduction of the ESR experiment, the eigenvalue spectrum is characterized by (a) four low-lying spin-doublets (including the ground state) and (b) an obvious and large energy gap above which (c) lie 12 closely bunched components of spin-quartet states, and finally, (d) above all these, spin doublets reappear over a wide energy range. Numerous calculations show how the low-lying doublets can fit the observed band at  $3900 \text{ cm}^{-1}$  but not features as high as  $8300 \text{ cm}^{-1}$ . So we assign the lowest transition as spin-allowed and the second as spin-forbidden. Decreasing the calculated energy gap between the four low doublets and the lowest energy quartets so as to reproduce the transition at  $8300 \text{ cm}^{-1}$  essentially determines  $e_{\sigma}(\text{O}, \text{N})$  and  $e_{\sigma}(\text{void})$  parameters uniquely and, indeed, tightens up almost all indeterminacy left by the ESR analysis. At the same time, the next lowest lying spin-allowed transitions are computed to lie at  $18800 \text{ cm}^{-1}$  and beyond in apparent agreement with the reported intense spectral features there (although intensity from charge-transfer transitions no doubt contributes to the high energy

**Table I.** Parameter Sets<sup>a</sup> Yielding Optimal Reproduction of Observed ESR  $g$  Tensors and d–d Transition Energies

parameter	Co(salen)	Co(clamben)
$F_2/\text{cm}^{-1}$	580 (20)	400 (20)
$F_4/\text{cm}^{-1}$	90 (5)	90 (5)
$\zeta/\text{cm}^{-1}$	210 (10)	225 (25)
$k$	0.73 (0.03)	1.00 (0.05)
$e_{\sigma}(\text{N}, \text{O})/\text{cm}^{-1}$	7100 (100)	7500 (100)
$e_{\pi  }(\text{O})/\text{cm}^{-1}$	2500 (100)	0 (100)
$e_{\sigma}(\text{void})/\text{cm}^{-1}$	–5000 (50)	–3750 (50)
$e_{\pi\perp}(\text{N}, \text{O})/\text{cm}^{-1}$	–420 (60)	–550 (50)
$e_{\pi  }(\text{O})/\text{cm}^{-1}$	300 (100)	0 (20)

<sup>a</sup> Estimated errors given in parentheses correspond to bounds outside of which agreement with observed data is unacceptably poor.

**Table II.** Comparisons between Observed  $g$  Tensors, Susceptibilities, and d–d Transition Energies and Those Calculated with the Optimal Parameter Sets of Table I

Transition Energies <sup>a</sup> ( $\text{cm}^{-1}$ )					
Co(salen)			Co(clamben)		
spin mult <sup>b</sup>	calcd	obsd	spin mult <sup>b</sup>	calcd	obsd
2	18781	17000			
4	13874		2	19888	19000
4	13866		4	14471	
4	12675		4	14429	
4	12642		4	13639	
4	11489		4	13577	
4	11464		4	12647	
4	9859		4	12630	
4	9828		4	12460	
4	9625		4	12359	
4	9613	8300	4	12220	
4	8646		4	11213	11000
4	8632		4	11192	
2	3550	3900	2	2632	
2	740		2	2025	
2	531		2	1033	
2	0		2	0	

#### $g$ Values<sup>c</sup>

	Co(salen)		Co(clamben)		
	calcd	obsd	calcd	obsd	
$g_x$	3.78	3.81	$g_x$	1.97	2.01
$g_y$	1.58	1.66	$g_y$	2.57	2.67
$g_z$	1.66	1.74	$g_z$	1.90	1.98

#### Molecular Susceptibilities ( $\text{cgsu} \times 10^{-6}$ ) at 300 K for Co(clamben)

	calcd	obsd <sup>14</sup>
$K_x$	1258	1450
$K_y$	2703	2326
$K_z$	1157	1473

<sup>a</sup> Listed up to the first high-energy doublet components. <sup>b</sup> Refers to the spin multiplicity of which these Kramers' doublets are components. <sup>c</sup> Orientations as in text and in Figures 2 and 3.

region also). The final optimal parameter set for Co(salen) is given in Table I and comparisons between observed and calculated d–d transition energies and ESR  $g$  values are made in Table II.

**The Clamben Complex.** The principal molecular  $g$  values in this system have been determined<sup>12</sup> as  $g_y = 2.67$ ,  $g_x = 2.01$ , and  $g_z = 1.98$ , and the axis labeling has been determined by comparison with the observed<sup>14</sup> susceptibility tensor, as discussed above. The parameter set chosen here comprised  $\bar{e}_{\sigma}(\text{N})$ ,  $e_{\sigma}(\text{void})$ , and  $\bar{e}_{\pi\perp}(\text{N})$  for the ligand field, together with  $F_2$ ,  $F_4$ ,  $\zeta$ , and  $k$  as before. Reproduction of the observed  $g$  tensor with this smaller parameter set was straightforward, in marked contrast to the difficult analysis of the salen complex. As in the latter study, wide ranges of all parameter values were investigated and low values of the electron-repulsion parameters were required to calculate  $g$  values of the correct order of magnitude. The correct pattern of  $g$  values, in particular that  $g_y$  is now the largest, emerges directly from all

(18) Gerloch, M.; Hanton, L. R.; Manning, M. R. *Inorg. Chem. Acta* **1981**, *48*, 205.

(19) Gerloch, M.; Slade, R. C. *Ligand-Field Parameters*; Cambridge University Press: Cambridge, U.K. 1973.

(20) Ferguson, J. *Prog. Inorg. Chem.* **1970**, *12*, 159.

(21) Ferguson, J.; Wood, D. L. *Aust. J. Chem.* **1970**, *23*, 861.

(22) Ceulemans, A.; Dendoover, M.; Vanquickenborne, L. G. *Inorg. Chem.* **1985**, *24*, 1153.

(23) Hitchman, M. A. *Inorg. Chem.* **1977**, *16*, 1985.

**Table III.** Orbital Energies (cm<sup>-1</sup>) Corresponding to the Optimal Parameter Values of Table I

	Co(salen) <sup>d</sup>	Co(clamben) <sup>e</sup>
orbital energies	25601 (a <sub>2</sub> )	23949 (a <sub>2</sub> )
	4534 (a <sub>1</sub> ) <sup>a</sup>	2270 (a <sub>1</sub> ) <sup>b</sup>
	3013 (b <sub>2</sub> )	1375 (a <sub>1</sub> ) <sup>a</sup>
	2794 (b <sub>1</sub> )	556 (b <sub>2</sub> )
	0 (a <sub>1</sub> )	0 (b <sub>1</sub> )
$\Delta E_{xz,yz}$ <sup>c</sup>	219	556

<sup>a</sup> Corresponds essentially to d<sub>x<sup>2</sup>-y<sup>2</sup></sub>. <sup>b</sup> Corresponds essentially to d<sub>z<sup>2</sup></sub>. <sup>c</sup> The separation between b<sub>1</sub> and b<sub>2</sub> levels (in C<sub>2v</sub> speciation) corresponds approximately to the orbital separation  $|E(d_{xz}) - E(d_{yz})|$ . <sup>d</sup> The corresponding d<sup>7</sup> ground state is |<sup>2</sup>B<sub>2</sub>;d<sub>yz</sub>⟩, and |<sup>2</sup>A<sub>1</sub>;d<sub>x<sup>2</sup>-y<sup>2</sup>⟩ lying some 1000 cm<sup>-1</sup> higher. <sup>e</sup> The d<sup>7</sup> ground state is |<sup>2</sup>A<sub>1</sub>;d<sub>z<sup>2</sup>⟩.</sub></sub>

computations. As only the {e} parameters carry any information on the nonspherical part of the metal environment and all nitrogen donors have common e<sub>λ</sub> parameter values, the ready selection of the molecular y direction can only result from the inexactitude of the square-planar coordination. From Figure 3, however, we note how little is the departure from 4-fold symmetry, pointing up once more the extreme sensitivity of ligand-field calculations for planar d<sup>7</sup> systems.

The region of parameter space yielding good fit with the ESR experiment is rather broad though by no means uninformative. As with the salen system, however, consideration of the optical d-d spectrum focused the analysis to an essentially unique optimal parameter set. While there appears to be no report of the transition energies of the clamben complex itself, absorption bands have been observed<sup>24</sup> for the closely analogous amben complex (whose structure differs only by lack of the chlorine substituent on each C<sub>6</sub> ring of the ligand). Here weak features around 11 000 cm<sup>-1</sup> and strong ones at 19 000 cm<sup>-1</sup> and above are taken to correspond with those at 8300 and 17 000 cm<sup>-1</sup> in the salen system and they have been reproduced as spin-forbidden and spin-allowed (and/or charge-transfer) transitions, respectively. The virtually unique optimal parameter set is given in Table I and comparisons with experimental ESR and optical spectral data are presented in Table II. Also included in that table is a comparison with the reported<sup>14</sup> molecular paramagnetic susceptibilities.

Finally, for the sake of the discussion to follow, we performed several calculations with e<sub>π<sub>||</sub>(O)</sub> ≠ 0. Good reproduction of experiment is possible (with the remaining parameter values as above) only for e<sub>π<sub>||</sub>(O)</sub> lying in the range 0 to -100 cm<sup>-1</sup>. Outside that range, computed principal g values no longer lie close to the Cartesian axes in Figure 3.

## 5. Discussion

The g tensors of representative examples of CoO<sub>2</sub>N<sub>2</sub> and CoN<sub>2</sub>N'<sub>2</sub> planar-coordinated, low-spin complexes have been satisfactorily reproduced within CLF models of the ligand-field. The primary difference between these ESR data is the interchanged roles of the in-plane directions for the large principal g value. That difference is reproduced in the model with a value for e<sub>π<sub>||</sub>(O)</sub> of some 25% of  $\bar{e}_\sigma(\text{O,N})$  in the CoO<sub>2</sub>N<sub>2</sub> system but a value near zero in the CoN<sub>2</sub>N'<sub>2</sub> system. Using the same sets of "best-fit" parameter values within a d<sup>1</sup> basis highlights two features (Table III). The splittings of the d<sub>xz</sub> and d<sub>yz</sub> orbital pair, arising from a potential whose source is electron density, is some 200 to 600 cm<sup>-1</sup> only: this is in sharp contrast to the 5000 and 10 000 cm<sup>-1</sup> splittings deduced by Ceulemans et al.<sup>22</sup> within their unphysical<sup>9</sup> "phase-coupled" model. Second, the ground state revealed in the salen complex involves the unpaired electron housed predominantly in the d<sub>yz</sub> orbital, in good agreement with the conclusions of an ENDOR study<sup>23</sup> of this system. It is clear that the correct ordering of g<sub>z</sub> > g<sub>y</sub> in that molecule is directly associated with this choice of ground state.

A somewhat detailed view of the electron distribution in these planar, low-spin cobalt(II) complexes can be constructed from

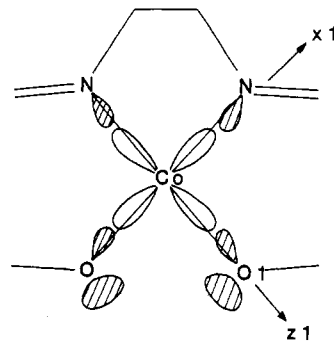


**Figure 4.** Local frame defined for the interaction between cobalt and ligand O1. With respect to the local frame, ring strain effects are expected to make a negative contribution to e<sub>π<sub>||</sub>(O)</sub> while the lone-pair contribution will be positive. Both features will make positive contributions to e<sub>π<sub>||</sub>(O)</sub>.

the foregoing analyses and our conclusions form under two headings concerning misdirected valency and central-field effects.

In Figure 4 is shown schematically the likely nature of the misdirected valency in Co(salen). Two contributions to the locally off-diagonal ligand field are possible by virtue of the nonbonding lone pair on the oxygen donors and of the bent bonding to be expected when intrachelate Co-N-C and Co-O-C angles are so wide. Considering the Co-O interaction, these two distinct sources for e<sub>π<sub>||</sub>(O)</sub> lie on opposite sides of the Co-O vector and so numerators of eq 5 for each will take opposite signs. The present calculations used locally defined axes as shown in Figure 4, and so the positive sign for e<sub>π<sub>||</sub>(O)</sub> determined by the analysis implies the dominance of the lone-pair contribution over that due to bent bonding, because the summation in eq 5 implies some net cancellation by these two mechanisms. This general view is supported by our finding in Co(clamben), which lacks the lone-pair effect, that e<sub>π<sub>||</sub>(O)</sub> is small and negative, if not zero. We suppose that the greater magnitude of the lone-pair contribution in the salen system arises partly out of the diffuseness and lateral spread and partly from the higher energy (with a consequently smaller value of (ε<sub>d</sub> -  $\bar{\epsilon}_\chi$ ) in (5)) of these nonbonding electrons compared with that of a bonding pair. The resultant magnitude of e<sub>π<sub>||</sub>(O)</sub> at 20–25% of e<sub>σ</sub>, though crucial in the reproduction of the observed ESR data, is only modest anyhow. No energetically close "π" orbitals lie in the plane of the salen (or clamben) ligands, of course, and so e<sub>π<sub>||</sub></sub> would normally expected to be zero. The CLF analysis of Co(clamben) successfully reproduced an experiment with that supposition. Yet an important characteristic of the Co(salen) study was the requirement for e<sub>π<sub>||</sub>(O)</sub> > 0 in order to reproduce the secondary g tensor anisotropy correctly. As discussed in section 2, this diagonal ligand-field parameter arises from the general misdirected valency. However, since the numerators of diagonal CLF parameters are necessarily positive, the positive value determined here for e<sub>π<sub>||</sub>(O)</sub> implies a positive denominator in (3) and hence that ε<sub>d</sub> >  $\bar{\epsilon}_{1,p}$ , as would, in any case, be expected for an occupied orbital. The same denominator (or denominators if we include the bent-bonding effect as well) occurs in (5), confirming the self-consistency of the model insofar as the signs and definitions of the various contributions to e<sub>π<sub>||</sub></sub> are concerned. Altogether, the analysis provides a clear demonstration of the ligand-field effect of nonbonding lone pairs; though suspected before and often compatible with prior analyses, we believe this is the first unequivocal demonstration of the phenomenon.

The ligand-field analyses of both complexes, in common with those of other low-spin, high-field systems, recognize very large nephelauxetic effects.<sup>19,26,27</sup> The ratios F<sub>2</sub>/F<sub>2</sub>(free ion) for salen and clamben molecules are 0.41 and 0.28, respectively. The corresponding ratios for F<sub>4</sub>/F<sub>4</sub>(free ion) are less reduced, as also found<sup>20,21</sup> in several high-spin complexes, but at 0.82 for each, very much so. It is interesting, though we do not believe dis-

(24) Green, M.; Tasker, P. A. *J. Chem. Soc. A* **1970**, 3105.

(25) Schweiger, A. *Struct. Bonding (Berlin)* **1982**, 51, 84.

(26) Jørgensen, C. K. *Prog. Inorg. Chem.* **1962**, 4, 73.

(27) Jørgensen, C. K. *Modern Aspects of Ligand-Field Theory*; North-Holland: Amsterdam, 1971.

quieting,<sup>31</sup> to note that the best-fit interelectron repulsion factors in the clamben complex imply a negative value for Racah's  $B$  parameter. The small Condon-Shortley parameters together with the large reduction in the effective spin-orbit coupling coefficient both reflect a considerable radial expansion of the  $d$  orbitals in these complexes with respect to the free ion. This accords well with the large  $e_{\sigma}$  values observed through the operation of the electroneutrality principle. Thus it appears that the adoption of a low-spin configuration, involving some migration of  $d$  electrons to regions lying between and above the primary metal-ligand bonds, facilitates a closer approach of the ligands—obviously in a synergic fashion. The consequently augmented donation of negative charge from the ligands reduces the effective nuclear charge on the metal and this is reflected in the reduced  $F_2$ ,  $F_4$ , and  $\zeta$  values as the  $d$  electron cloud expands.<sup>32</sup> At the same time, the increased  $\sigma$  donation from the salen and clamben chelates depletes the ligand electron density to the point that their usual (that is, within high-spin complexes) role as  $\pi$  donors is markedly decreased and possibly reversed; both analyses are characterized by small, negative  $e_{\pi\perp}(\text{O})$  parameter values.

Comparison of the  $e_{\sigma}$  and  $e_{\pi\perp}$  values between the two complexes reveals greater  $\sigma$ -donor and  $\pi$ -acceptor roles of the imine ligands than of the salicylidene oxygens. A relatively enhanced electron donation to the metal atom in the clamben system is associated with a greater nephelauxetic effect as evidenced by the smaller value of  $F_2$ . These same trends appear to account for the much reduced ligand-field contribution of the coordination voids in the clamben complex also. Thus we expect that while lower-lying and more strongly bonding metal  $s(p)$ -ligand interactions characterize the clamben system, the "bond orbitals"<sup>3,8</sup> associated with the voids will be more  $s$ -like and less well bound, resulting in a diminished interaction with the  $d_{z^2}$  orbital of the metal. As the values of  $e_{\sigma}(\text{void})$  are determined empirically largely by fitting the spin-forbidden bands at 8300 and 11 000  $\text{cm}^{-1}$  in the salen and clamben complexes, respectively, these spectral features are to be seen as the direct manifestation of the changing character of the "residual" orbitals associated with the coordination voids. This proposal is clearly one that deserves further investigation in future studies.

The large nephelauxetic effect observed in these and other low-spin complexes invites a fresh appraisal of the factors governing the selection of high- and low-spin forms by complexes in general. The established view rests upon the arguments Griffith<sup>28</sup>

applied to octahedral complexes in which the spin state adopted depends upon the relative magnitudes of ligand-field and electron-pairing energies,  $\Delta$  and  $\Pi$ . The pairing energy is presumed to be greater in the low-spin arrangement. This is certainly true if these energies are expressed in units of the interelectron repulsion parameters  $F_2$  and  $F_4$  (or  $B$  and  $C$ , as desired). However, the gross reduction observed in these parameters for low-spin complexes (which we surmise to be a general feature) adds a second layer to the " $\Delta$  vs.  $\Pi$ " concept in that the change in pairing energy expressed in terms of wavenumbers (e.g.) will be much less than as first envisaged and, indeed, could be a decrease in principle. We shall report on this proposition elsewhere.

The ligand-field effects of misdirected valence are pursued in the following two papers.

**Acknowledgment.** We are most grateful to Dr. M. A. Hitchman for his critical appraisal of this work and for drawing our attention to the ENDOR experiment quoted in ref 25. R.J.D. acknowledges the award of a Commonwealth Scholarship and support of the British Council. M.J.D. acknowledges the support of an award of the Science and Engineering Research Council.

**Registry No.** Co(salen), 14167-18-1; Co(clamben), 36870-52-7.

- (28) Griffith, J. S. *J. Inorg. Nucl. Chem.* **1956**, *2*, 1.
- (29) Contributions from metal core electrons do, of course, arise and are manifest in the defining potential of the  $d$  functions but explicitly excluded from the cellular potentials that ultimately contribute only to the globally nonspherical ligand-field potential.
- (30) The association of a positive  $e_{\pi\sigma}$  parameter with misdirected valency in the negative  $xz$  quadrant may be deduced alternatively by examination of the phases of the equivalent potential expressed as a superposition of spherical harmonics (of the local  $Y_1^2$  and  $Y_1^4$ ) for ligand-field sources displaced off-axis in the given frame, followed by rotation.
- (31) Racah's  $B$  parameter is related to the difference between intrinsically positive Slater-Condon-Shortley parameters.
- (32) The large reductions in interelectron repulsion parameters and spin-orbit coupling coefficient both attest a much reduced effective nuclear charge and large nephelauxetic effect. The small orbital reduction (large  $k$  values) in the magnetic moment operators is *not* in conflict with these findings within the modern interpretation of ligand-field theory, as discussed in section 11.7 of ref 3 or in ref 2, for example. Only within the incorrect view of ligand-field theory as a division of molecular-orbital theory, does one expect reductions in Condon-Shortley and spin-orbit coupling parameters to be accompanied by qualitatively similar reductions in Stevens' orbital reduction factor.

Contribution from the University Chemical Laboratory,  
Cambridge CB2 1EW, U.K.

## Ligand Fields from Misdirected Valency. 2. Bent Bonding in Copper(II) Acetylacetonates<sup>†</sup>

Robert J. Deeth, Melinda J. Duer, and Malcolm Gerloch\*

Received December 5, 1986

Analyses of the  $d-d$  spectra of  $\text{Cu}(\text{3-methylacac})_2$ ,  $\text{Cu}(\text{acac})_2$ ,  $\text{Cu}(\text{phenoxycarbonyl}(\text{acac}))_2$ ,  $\text{Cu}(\text{3-phenylacac})_2$ , and  $\text{Cu}(\text{acac})_2(\text{quinoline})$  ( $\text{acac} \equiv \text{acetylacetonate}$ ) have been performed within the cellular ligand-field (CLF) model. A coherent view of the bonding electron distribution within the series has been formed and the ligand-field analyses consistently recognize the contribution of coordination voids as well as misdirected valence between metal and chelate deriving from ligand tilting, ring strain, and the role of the nonbonding oxygen lone pairs.

### 1. Introduction

The  $d$  orbital splittings in copper(II) acetylacetonates have been the focus of repeated ligand-field studies and have generated an extensive literature with respect to the use of vibronic selection rules in the assignment of  $d-d$  spectra in planar, centrosymmetric chromophores. A comprehensive review<sup>1</sup> in 1972 by Smith, together with more recent work, has established two main contenders

for the assignments in copper(II) acetylacetonates, which are principally differentiated by their (implicit) inclusion or exclusion of ligand-field contributions<sup>2-4</sup> from the coordination voids above and below the molecular planes. The importance of that con-

<sup>†</sup> No reprints available from this laboratory.

- (1) Smith, D. W. *Struct. Bonding (Berlin)* **1972**, *12*, 49.
- (2) Gerloch, M.; Harding, J. H.; Woolley, R. G. *Struct. Bonding (Berlin)* **1981**, *46*, 1.
- (3) Gerloch, M. *Magnetism and Ligand-Field Analysis*; Cambridge University Press: Cambridge, U.K., 1983.
- (4) Gerloch, M.; Woolley, R. G. *Prog. Inorg. Chem.* **1983**, *31*, 371.